Chinese Chemical Letters 33 (2022) 3429–3434

Contents lists available at ScienceDirect

Chinese Chemical Letters

journal homepage: www.elsevier.com/locate/cclet

Efficient separation between trivalent americium and lanthanides enabled by a phenanthroline-based polymeric organic framework

Afshin Khayambashi[a,1], Long Chen[a,1], Xue Dong[b], Kai Li[a], Zhipeng Wang[b], Linwei He[a], Suresh Annam[a], Lixi Chen[a], Yaxing Wang[a], Matthew V. Sheridan[a], Chao Xu[b], Shuao Wang[a,*]

[a] State Key Laboratory of Radiation Medicine and Protection, School for Radiological and Interdisciplinary Sciences (RAD-X) and Collaborative Innovation Center of Radiation Medicine of Jiangsu Higher Education Institutions, Soochow University, Suzhou 215123, China
[b] Institute of Nuclear and New Energy Technology, Tsinghua University, Beijing 100084, China

ARTICLE INFO

Article history:
Received 27 November 2021
Revised 29 January 2022
Accepted 5 February 2022
Available online 9 February 2022

Keywords:
Porous organic framework
Americium
Lanthanides
Separation
Stability

ABSTRACT

Separation of the minor actinides (Am and Cm) from lanthanides in high-level liquid wastes (HLLW) is one of the most challenging chemical separation tasks known owing to their chemical similarities and is highly significant in nuclear fuel reprocessing plants because it could practically lead to sustainable nuclear energy by closing the nuclear fuel cycle. The solid phase extraction is proposed to be a possible strategy but all reported sorbent materials severely suffer from limited stability and/or efficiency caused by the harsh conditions of high acidity coupled with intense irradiation. Herein, a phenanthroline-based polymeric organic framework (PhenTAPB-POF) was designed and tested for the separation of trivalent americium from lanthanides for the first time. Due to its fully conjugated structure, PhenTAPB-POF exhibits previously unachieved stability under the combined extreme conditions of strong acids and high irradiation field. The americium partitioning experiment indicates that PhenTAPB-POF possesses an ultrahigh adsorption selectivity towards Am(III) over lanthanides (*e.g.,* $SF_{Am(III)/Eu(III)} = 3326$) in highly acidic simulated HLLW and relatively fast adsorption kinetics in both static and dynamic experiments. Am(III) can be almost quantitatively eluted from the PhenTAPB-POF packed-column using a concentrated nitric acid elution. The high stability and superior separation performance endow PhenTAPB-POF with the promising alternative for separating minor actinides over lanthanides from highly acidic HLLW streams.

Nuclear energy with an advanced nuclear fuel cycle is a primary clean energy source as a sustainable solution for the increasing global electricity demand [1,2]. However, environmental issues such as nuclear waste handling and disposal associated with the used fuel reprocessing have been of significant concerns [3]. In the closed nuclear fuel cycle, uranium (U) and plutonium (Pu) can be recovered from the uranium dioxide used fuel by the PUREX (plutonium and uranium recovery by extraction) process [4]. The minor actinides (MA: Am, Np and Cm) and some fission products (*e.g.,* ^{99}Tc, ^{135}Cs) are the long-term radiotoxicity elements in the high-level liquid waste (HLLW) that remain from the PUREX process [5]. Most of the current feasible strategies in the nuclear fuel cycle call for the permanent disposal of the remained wastes vitrificated in a glass form inside the metal containers in a geological repository. In contrast, the advanced nuclear fuel cycles advocate the partitioning & transmutation strategy (P&T), which separates the long-lived MA and FP from HLLW and then transmutes them to stable or short-lived radionuclides. This technique employing an accelerator-driven subcritical system (ADS) minimizes the nuclear waste's volume and radiotoxicity [5,6]. The oxygen donor ligands such as CMPO [7], TRPO [8], and DMDOHEMA [9] using solvent extraction (SE) can sequestrate MA(III) and Ln(III) together from fission products in HLLW. Minor actinides also need to be partitioned from the lanthanides before the transmutation process due to certain lanthanides' high neutron absorption cross-sections such as Sm, Eu, and Gd [10]. However, the MA(III) and Ln(III) separation is still a significant challenge because of their similar ionic radii, charge density, and coordination modes, in addition to the large excess of Ln(III) compared with MA(III) in HLLW [11].

The ligands containing soft N-donor atoms have been introduced to possess the ability to discriminate between MA(III) and Ln(III) [12]. The covalency between minor actinides (5f elements)

* Corresponding author.
E-mail address: shuaowang@suda.edu.cn (S. Wang).
[1] These authors contributed equally to this work.

https://doi.org/10.1016/j.cclet.2022.02.011
1001-8417/

and the ligand or adsorbent with nitrogen donors' sites is more significant than that in lanthanides (4f elements) complexes based on the hard and soft Lewis acid-base theory, which fiercely relies on the number of possible coordination sites in the ligand [13]. At present, the pyridine-based N-donor ligands such as 2,6-bis(5,6-dialkyl-1,2,4-triazin-3-yl)pyridines (BTPs) [14,15] and 6,6′-bis(5,6-dialkyl-1,2,4-triazin-3-yl)-2,2′-bipyridines (BTBPs) [16,17] are reported as the potential ligands for the MA/Ln partitioning. These ligands in solvent extraction technique could separate Am and Eu with a high separation factor (SF Am/Eu > 100) in nitric acid media ranging pH level to molar concentrations. However, using these ligands in solvent extraction faces the following drawbacks: the *i*-Pr-BTP and $CyMe_4$-BTBP exhibit poor solubility properties in traditional solvents, *n*-alkylated BTPs and BTBPs are chemically unstable under irradiation in nitric acid solution, CA-BTP reveals a low loading capacity, and $CyMe_4$-BTP displays a poor stripping performance and slow kinetics [18]. Moreover, a tetradentate phenanthroline ligand [19] and 2,9-diamide-1,10-phenanthroline (DAPhen) [20] in a typical ionic liquid ($C_4mimNTf_2$) reveal insufficient extraction properties towards both Am and Eu in the highly acidic solutions (>0.1 mol/L HNO_3). Even though solvent extraction is the preoccupant technique in MA(III)/Ln(III) separation, the significant limitations are worthy of paying more attention, such as large amounts of (toxic, volatile, and explosive) organic solvent, hydrolytic and radiolytic degradation of the extractants and solvents, third phase formation, multi-stage extraction procedures and large volumes of secondary HLLW [21,22].

To overcome the disadvantages mentioned above, developing a solid-phase extraction technique by impregnating extractant solutions into the pores of macroporous inorganic or polymeric substrates has received considerable attention [23,24]. Wei *et al.* introduced a series of solid-phase extractants by impregnating various ligands such as BTPs, isoHex-BTP, and Me_2-CA-BTP into the stable microporous silica/polymer composite support (SiO_2-P particles) [25–28]. Me_2-CA-BTP/SiO_2-P exhibits a good adsorption selectivity towards Am(III) over Eu(III) (SF Am/Eu over 75) in a wide range of nitric acid concentrations (1–3 mol/L) [29]. However, using the physical impregnation technique to synthesize the adsorbent has raised legitimate concerns over these materials' stability against radiation damage and acid hydrolysis [30]. Besides, these impregnated silica-based adsorbents or functionalized mesoporous silica-supported materials [31,32] are not entirely combustible to gaseous products to adhere to the CHON principle. Ultimately, these limitations undermine solid-phase extraction processes using these materials for nuclear reprocessing applications.

The adsorption technique using the radiation-resistant covalent bonded materials with selective binding sites can defeat these limitations while holding the merits in partitioning minor actinides from HLLW in view of significant insolubility and stability in acidic solutions [33]. Porous organic materials (POMs) with high thermal and chemical stability, lightweight, and excellent structure tunability have been considered potential candidates for separation processes in different applications [34]. A large family of POM materials, including covalent-organic frameworks (COFs) [35], porous aromatic frameworks (PAFs) [36], polymers of intrinsic microporosity (PIMs) [37], covalent triazine frameworks (CTFs) [38], and porous organic frameworks (POFs) [39], have been developed through various chemical reactions such as Suzuki cross-coupling reaction, Schiff-base reaction, Sonogashira-Hagihara reaction, Friedel-Crafts arylation, cyclotrimerization, and Yamamoto reaction [39–41]. Although most of these materials are stable under acidic conditions, none has been reported for an applicable MA/Ln separation in highly acidic conditions. For example, a carboxylic acid-functionalized porous aromatic framework (PAF-BPP-7: Berkeley porous polymer-7) displays the maximum adsorption efficiency up to 50% and 88% for Am^{3+} and Dy^{3+} respectively in low pH conditions, which should be further improved to achieve promising MA and Ln group adsorption or MA/Ln separation [30]. Accordingly, great efforts are demanded to design and synthesize appropriate N-donor porous organic materials for MA/Ln separation. Phenanthroline-based ligands such as BTPhens have been considered a potential material in both solvent and solid-phase extraction techniques due to their excellent ability to separate trivalent actinides and lanthanides with much better adaptability to highly acidic conditions compared with the pyridine-based materials [42,43]. The *cis*-locked phenanthroline juxtaposes the nitrogen donors, which gives rise to the more rapid and thermodynamically favored formation of the ligand-metal complex [44].

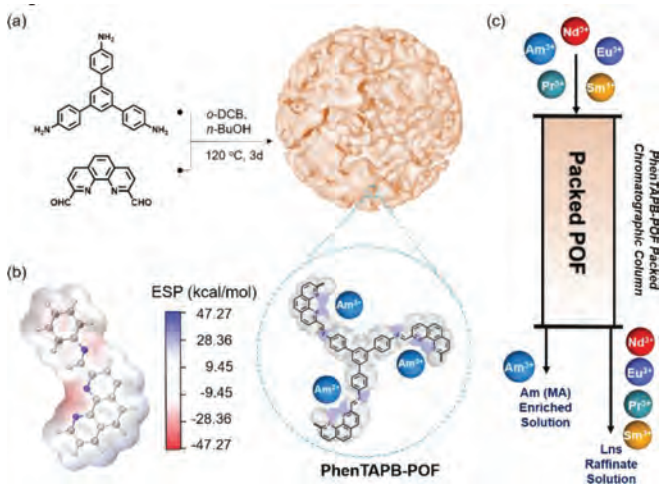

Fig. 1. (a) The synthetic route for PhenTAPB-POF. (b) The simulation of the electrostatic potential (ESP) distribution of the 1,10-phenanthroline units in the synthesized POF framework. (c) The schematic of the chromatography column separation system packed by PhenTAPB-POF for MA and Lns separation.

In this contribution, the idea of introducing a simple phenanthroline-based ligand as the building blocks of imine-linked microporous polymer organic frameworks (POFs) came up due to the proposed potential of Phen-POF materials for MA/Ln separation under extreme conditions as well as its simple synthesis procedure for an industrial scale with no post-synthetic modification or functionalization. It has been well-documented that Schiff-base reaction as a high-yielding approach is a versatile tool in synthesizing porous organic architectures that the process is a one-pot condensation reaction and does not involve expensive catalysts [45]. Note that Phen-POFs are only composed of C, H, O and N, which are advantageous to nuclear waste management based on the CHON principle since they are entirely combustible to gaseous products, resulting in less secondary radioactive waste. In this study, we demonstrate the introduction of a POF material for MA/Ln separation for the first time, which was synthesized by the imine condensation of 1,10-phenanthroline-2,9-dicarbaldehyde with 1,3,5-tris(4-aminophenyl)benzene (Fig. 1a). The resultant PhenTAPB-POF adsorbent with partial negative electrostatic potential (Fig. 1b) exhibits significant chemical stability against irradiation and highly acidic conditions and demonstrates selective adsorption for Am(III) over lanthanides in static and dynamic experiments (Fig. 1c).

PhenTAPB-POF was synthesized with 10-phenanthroline-2,9-dicarbaldehyde and 1,3,5-tris(4-aminophenyl)benzene (TAPB) under an acid-catalyzed solvothermal process (Fig. 1a). To validate the formation of POF material, the obtained red-brown PhenTAPB-POF and its two reactants were characterized by Fourier transform infrared (FT-IR) spectrometry, as shown in Fig. 2a. The characteristic peaks of TAPB at 3457, 3317, and 3202 cm^{-1} represent the stretching vibration of the N–H bond in amino functional group, and the

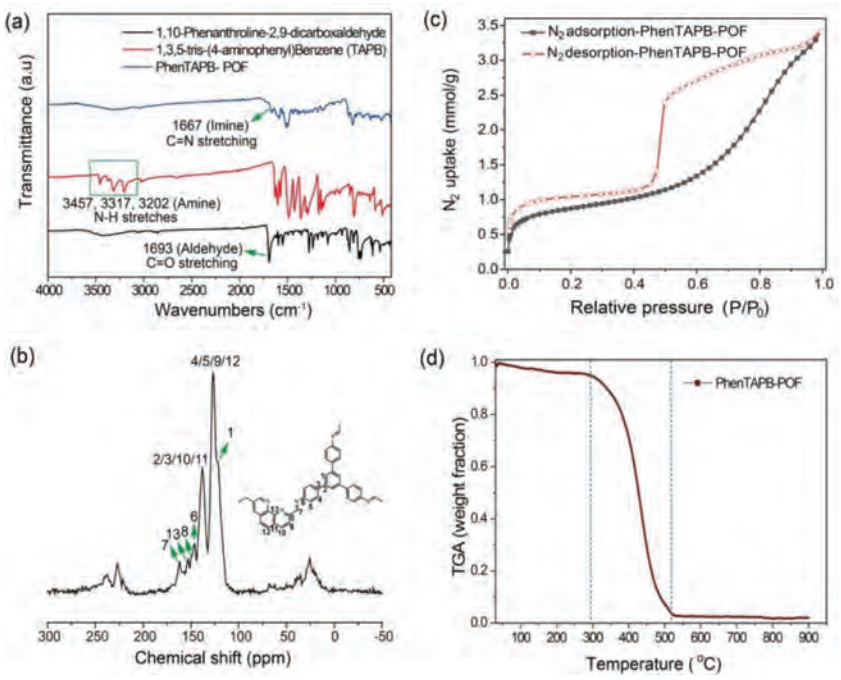

Fig. 2. (a) FT-IR spectra of 1,10-phenanthroline-2,9-dicarbaldehyde (Phen), 1,3,5-tris(4-aminophenyl) benzene (TAPB) and synthesized PhenTAPB-POF. (b) The ^{13}C solid-state NMR spectrum result of PhenTAPB-POF. (c) The N_2 adsorption and desorption isotherms of PhenTAPB-POF. (d) The TGA profile of PhenTAPB-POF under O_2 atmosphere.

peak at 1693 cm^{-1} for 10-phenanthroline-2,9-dicarbaldehyde is attributed to the C=O stretching band (aldehyde). In the IR spectra of PhenTAPB-POF, a characteristic peak of C=N stretching vibration appearing at 1667 cm^{-1} indicates the formation of an imine linkage which is accompanied by the absence of the peaks from the aldehyde and amino stretching vibrations [46]. The obtained results confirm a successful conversion of those two monomers into a Schiff-base POF polymer through a condensation reaction. Furthermore, the successful formation of PhenTAPB-POF is further corroborated by the solid-state ^{13}C NMR spectroscopy, which displays resonances associated with the imine group at 161.5 ppm, as shown in Fig. 2b [47].

N_2 adsorption-desorption isotherms (Fig. 2c) at 77 K were employed to verify the formation of a porous structure in PhenTAPB-POF, which displays the typical type IV isotherms. The hysteresis loop in the high relative pressure region represents a large number of micropores and mesopores features in PhenTAPB-POF [48]. The pore width distribution of PhenTAPB-POF adsorbent derived from the N_2 adsorption isotherm is also shown in Fig. S1 (Supporting information). The calculated Brunauer-Emmett-Teller (BET) surface area of 65.98 m^2/g indicates a moderate porosity, which may be caused by the staggered stacking of layers hindering the required migration of nitrogen into the material [49]. The scanning electron microscopy (SEM) image (Fig. S3a in Supporting information) and the powder X-ray diffraction (PXRD) pattern (Fig. S2 in Supporting information) of PhenTAPB-POF show the surface morphology and amorphous structure of the material, respectively.

Thermal gravity analysis (TGA) under an oxygen atmosphere is used to ensure the thermal stability of the synthesized adsorbent in relevant high temperatures and further clarify the CHON principle of the promising PhenTAPB-POF adsorbent by combusting the polymeric adsorbent completely to gaseous products. TG curve in Fig. 2d indicates that the PhenTAPB-POF has two regions of weight loss towards the increase in temperature. The first region is a negligible weight loss from ambient temperature to 150 °C, attributed to the rapid evaporation of the residual solvents and adsorbed water [50]. The second region stands for the temperature range of 300–550 °C, in which the weight loss sharply increases more than 95%, which ascribes to the complete decomposition of the POF framework. The TGA profile of the adsorbent reaches a plateau in the temperate ranges from 150 °C to 300 °C, indicating the thermal stability of PhenTAPB-POF.

The electrostatic potential (ESP) distribution of the 1,10-phenanthroline units in POF skeleton is shown in Fig. 1b. Due to the relatively high electronegativity of nitrogen atoms, the regions close to the N atoms of 1,10-position in the phenanthroline rings form the most negative ESP (red areas), which are appropriate for accommodating the electropositive Am^{3+}. Besides, the N atoms from amine linkage (-C=N-) also provide a relatively narrow negative region, which may have affinity for Am^{3+}.

The effect of nitric acid concentration on the adsorption of americium into the POF material is illustrated in Fig. 3a. Adsorption efficiency of americium gradually decreases with increasing the acidity from 0.01 mol/L to 0.5 mol/L HNO_3 and subsequently decreased sharply with a further increase of acidity to 3 mol/L. The reason is that the adsorption sites are likely to be protonated in a higher level of acidity, resulting in the decrease of available N-donor sites [51]. From another perspective, the adsorption mechanism towards Am(III) and HNO_3 can be described in Eqs. 1 and 2, respectively, which are derived from the extraction mechanism of the N-donor ligands [52].

$$Am^{3+} + 3NO_3^- + \text{PhenTAPB-POF} \rightarrow Am(\text{PhenTAPB-POF})(NO_3^-)_3 \quad (1)$$

$$xH^+ + xNO_3^- + \text{PhenTAPB-POF} \rightarrow \text{PhenTAPB-POF}{\cdot}xHNO_3 \quad (2)$$

Due to the americium's trivalent oxidation state, three NO_3^- ions are incorporated into the coordination sphere of Am(III) to maintain the neutral POF as the chemisorption shown in Eq. 1. Further increase in HNO_3 concentration may support the sorption of nitric acid as illustrated in Eq. 2, which decelerates the rate and efficiency of Am adsorption by lowering the concentration of free adsorption sites on PhenTAPB-POF. The obtained results reveal that

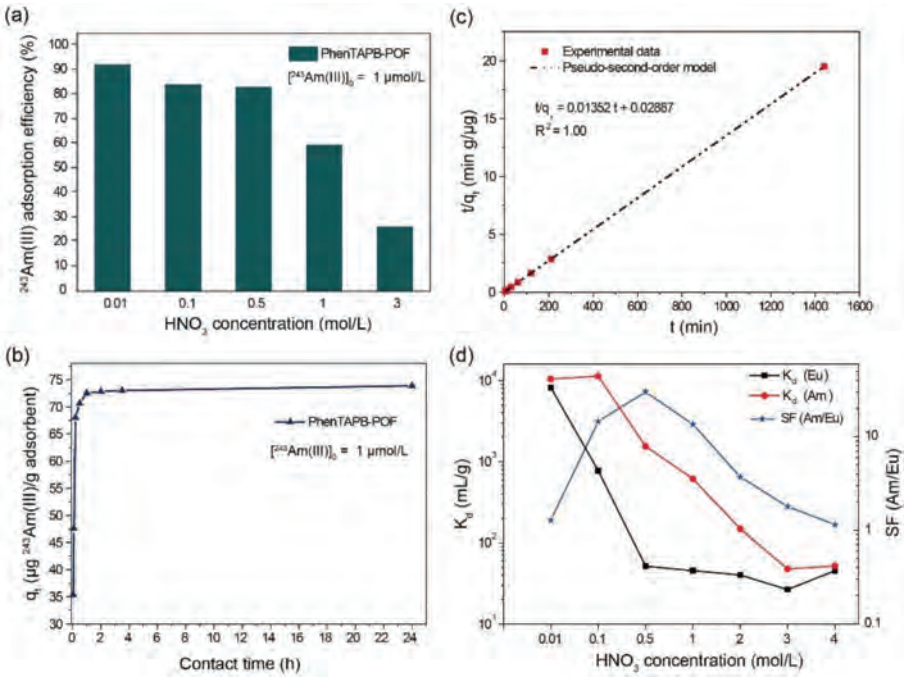

Fig. 3. (a) Variations of the americium adsorption efficiency of PhenTAPB-POF *versus* the nitric acid concentrations (mol/L) in a pure americium system (initial concentration of Am(III) = 1 μmol/L, contact time: 24 h, adsorbent dose: 5 mg/2 mL, at 25 °C). (b) Effect of contact time on americium adsorption onto PhenTAPB-POF in 0.5 mol/L nitric acid medium (initial concentration of Am(III) = 1 μmol/L, adsorbent dose: 5 mg /2 mL, at 25 °C). (c) *Pseudo*-second order plot used for kinetics study of the americium adsorption process. (d) Influence of HNO_3 concentration on the adsorption and separation of Am(III) and Eu(III) using PhenTAPB-POF (initial concentrations of Am(III) and Eu(III) = 1 μmol/L, contact time: 24 h, adsorbent dose: 2 mg/mL (4 mg/2 mL), at 25 °C).

Am(III) adsorption using the PhenTAPB-POF in nitric acid media with a concentration less than 0.5 mol/L is practically acceptable since the obtained adsorption efficiency is higher than 80%. Such a high adsorption efficiency for the americium extraction with a very low concentration (1 μmol/L) might be received by a highly negative enthalpy of adsorption (Δ_{Hads}) caused by the multiple chemical interactions between the americium ions and the binding sites [30]. It is worth noting that the adsorbent dose in the batch experiments is only 2, which means that only 2 mg of adsorbent is in contact with 1 mL of solution. The adsorbent dose is 10 times smaller than the performed adsorbent dose in the reported Me_2-CA-BTP/SiO_2-P adsorbent [18]. Therefore, increasing the adsorbent dose obviously could reach higher adsorption efficiency. The effect of contact time on Am(III) adsorption onto PhenTAPB-POF material was investigated in a 0.5 mol/L HNO_3 solution containing pure Am(III) with the initial concentration of 1 μmol/L, as shown in Fig. 3b. As a result, PhenTAPB-POF quickly adsorbs Am(III), reaching the equilibrium within 1 h. The adsorption kinetics has been investigated as shown in Fig. 3c with a linear plot of *"t/qt" versus "t"*, which represents that the pseudo-second-order model is appropriate to express the Am(III) adsorption onto the synthesized POF. The *pseudo*-second-order model indicates that the rate-limiting step of Am(III) adsorption might be controlled by a chemisorption mechanism involving valence forces through transfer, sharing, or exchange of electrons between Am(III) ions and PhenTAPB-POF [21]. The adsorption mechanisms might be attributed to inner sphere complexation [53,54]. As shown in Fig. S5 (Supporting information), the adsorption kinetics can not be described well using the *pseudo*-first-order model.

The static adsorption study was carried out to investigate the feasibility of PhenTAPB-POF material for the selective adsorption of Am(III) towards Eu(III) in a range of nitric acid concentrations, as shown in Fig. 3d. The static results reveal the optimum point of separation at 0.5 mol/L HNO_3 that the adsorbent exhibits significant adsorption towards Am(III) with the distribution coefficient of more than 1400 mL/g and the Am(III)/Eu(III) separation factor over 30. This optimized environment for separating minor actinides and lanthanides is assumed as a highly acidic condition suitable for practical application. Noting that the initial concentrations of both elements are of the same as 1 μmol/L to ensure the similar competing conditions for both elements, which has been missing in most of the published works. The selective adsorption of Am(III) over Eu(III) might be caused by the greater covalency in complexes between Am (as a 5f element) and ligand than that in complexes of Eu (as a 4f element) [55]. A shred of evidence for the covalence in the N-donor complex of Am(III) has been reported using NMR investigation exhibiting a large difference in nitrogen chemical shift for coordinating N-atoms in Am(III) complexes compared to that of both in free ligand and Ln(III) complexes [56]. Moreover, a batch adsorption experiment was employed to investigate the separation performance of the adsorbent for the simulated HLLW in which the concentration of the lanthanides is a thousand times higher than that of the americium. The illustrated results in Fig. 4a reveal the potential of PhenTAPB-POF to treat HLLW solutions. A slight decrease in Am(III) adsorption efficiency was observed compared to the adsorption results of the pure Am(III) system in Fig. 3a. However, the obtained significant separation factors for Am(III) towards lanthanides elements (*e.g.*, $SF_{Am(III)/Eu(III)} = 3326.7$) indicate the exceptional MA/Ln separation capability for the synthesized POF adsorbent.

To further evaluate the PhenTAPB-POF for the separation of MA(III) from lanthanides, a hot dynamic test using simulated HLLW containing 1 μmol/L Am(III) and 1 mmol/L of stable lanthanides (Ce, Pr, Nd, Sm, Eu, Gd, Tb, Dy, Ho and Er) in 0.5 mol/L HNO_3 was carried out at ambient temperature. The elution curves of americium and lanthanides were drawn by the obtained radioactivity measurement and ICP spectroscopy results, respectively, as shown in Fig. 4b. Chromatogram of PhenTAPB-POF shows almost no adsorption towards lanthanides in which these elements were eluted with the feed stream and the following 0.5 mol/L HNO_3 elution

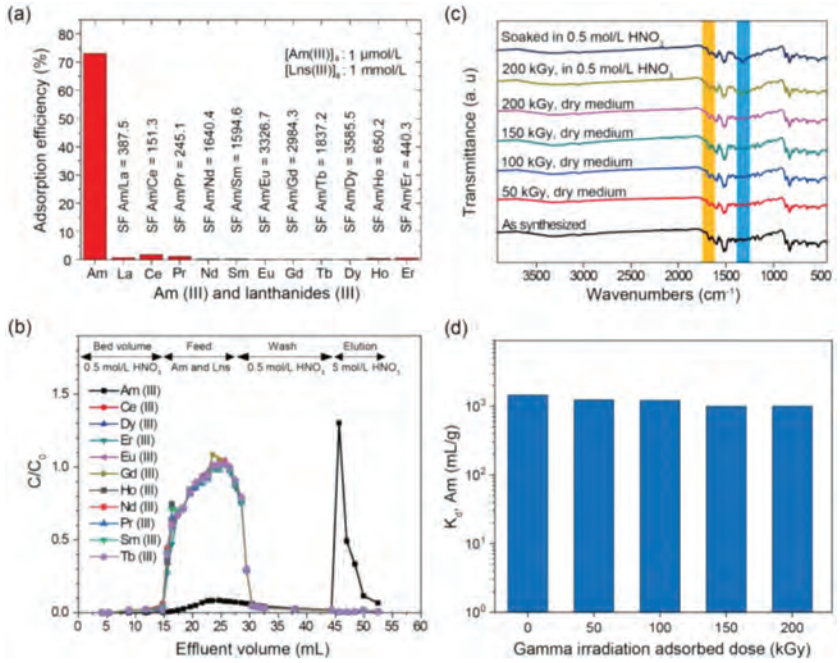

Fig. 4. (a) The Am(III) and Lns(III) adsorption efficiency and separation factors of PhenTAPB-POF in 0.5 mol/L HNO_3 (initial concentration of Am(III) = 1 μmol/L, Lns(III) = 1 mmol/L, contact time: 24 h, adsorbent dose: 5 mg /2 mL, at 25 °C). (b) Chromatographic separation of americium over lanthanides from a simulated HLLW using a PhenTAPB-POF packed column (flow rate of effluents: 1 mL/min, feed: 12 mL of simulated HLLW containing 1 μmol/L Am(III) and 1 mmol/L Lns(III) in 0.5 mol/L HNO_3 solution, column: a plastic column with an inner diameter of 7 mm and 25 mm in length which was packed in a dry state by 400 mg of PhenTAPB-POF adsorbent). (c) The FT-IR spectra of gamma-irradiated PhenTAPB-POF with the absorbed doses of 50, 100, 150, and 200 kGy in a dry medium and 200 kGy in a 0.5 mol/L nitric acid medium. Also, the IR spectra of treated PhenTAPB-POF in 0.5 mol/L HNO_3 for 10 days. (d) Effect of gamma irradiation on PhenTAPB-POF with the adsorbed doses of 50, 100, 150, and 200 kGy in a 0.5 mol/L HNO_3 medium towards the adsorption efficiency of americium ($[Am(III)]_0 = 1$ μmol/L, contact time: 24 h, adsorbent ratio: 2 mg/mL (4 mg /2 mL), in 0.5 mol/L HNO_3 single Am(III) solution at 25 °C).

solution. Meanwhile, Am is mainly adsorbed (more than 95%) by PhenTAPB-POF adsorbent. Then it was eluted well by using 5 mol/L HNO_3 as the elution agent of americium. In conclusion, a nearly complete separation between americium and lanthanides (as the typical fission products) has been achieved using a small column setup only including 400 mg of adsorbent with a relatively fast flow rate, which is a significant finding to consider PhenTAPB-POF as a promising phenanthroline-based adsorbent for the separation purposes in analytical and semi-industrial applications. The slight adsorption of americium is due to the short length of the column, which was designed to generate less radioactive waste in the laboratory.

PhenTAPB-POF exhibits significant resistance toward high-energy ionizing γ-rays in highly acidic conditions with the irradiation absorbed dose ranging from 50 kGy to 200 kGy, guaranteeing a substantial prerequisite for the application in HLLW treatment. To evaluate the chemical stability of PhenTAPB-POF, fresh samples were dispersed in nitric acid solutions with various levels of acidities for 10 days. The characteristic peaks, including the C=N stretching vibration in IR spectra of the treated samples in Fig. S4 (Supporting information), almost duplicate with those of the as-synthesized sample. The vibrational bands of the nitric acid adsorbed on POF appear at 1310 cm^{-1}, which further confirms the nitric acid adsorption onto PhenTAPB-POF [57]. Furthermore, the fully conjugated structure of adsorbent protects the chemical bonds from the strong doses of γ irradiation from a ^{60}Co radiation source (92.42 PBq, dose rate of 3.125 kGy/h) in dry and 0.5 mol/L nitric acid mediums. The radiation resistance is confirmed by FT-IR, PXRD, and SEM analyses of the irradiated samples. As can be seen, the FT-IR spectra (Fig. 4c), PXRD patterns (Fig. S2 in Supporting information), and microsphere morphology (Fig. S3 in Supporting information) of irradiated PhenTAPB-POF treated in highly acidic nitric acid solution remain almost unaffected. Moreover, decent radiation resistance of the adsorbent was further confirmed by the Am(III) adsorption onto the irradiated samples in 0.5 mol/L HNO_3 medium, as shown in Fig. 4d. The results indicate that the distribution coefficient of the Am(III) adsorption remains nearly unchanged after irradiation in acidic media which is indeed an outstanding feature for the minor actinides and lanthanides separation in real applications.

In summary, the phenanthroline-based polymeric organic adsorbent (PhenTAPB-POF) was constructed with rigid aromatic ligands using Schiff-base reaction and comprehensively characterized. The foregoing static and dynamic adsorption results signify the extensive potential of PhenTAPB-POF as a nitrogen donor framework for the separation of minor actinides over lanthanide from the simulated HLLW in a highly acidic solution (0.5 mol/L HNO_3) under robust gamma-ray irradiation (200 kGy). The synthesized PhenTAPB-POF is sufficiently stable in contact with nitric acid in a gamma source's radiation field and thermally stable up to 300 °C in the O_2 atmosphere. Moreover, this novel POF material can completely degrade into gaseous products in 550 °C, easing the waste management of the contaminated sorbents after use. These merits together cannot be achieved by any of the previously reported adsorbents such as the silica-based solid-phase extractants and other inorganic or polymeric materials and frameworks. A POF adsorbent with these outstanding advantages endows the family of POF, PAF, and COF materials with the promising potentials to solve the most severe issues in nuclear fuel cycles, such as the minor actinides and lanthanide separation, technetium removal, and cesium and strontium recovery.

Declaration of competing interest

The authors declare no conflict of interest.

Acknowledgment

This work was supported by the grants from the National Natural Science Foundation of China (Nos. 21825601, 21790374, and 21806117).

Supplementary materials

Supplementary material associated with this article can be found, in the online version, at doi:10.1016/j.cclet.2022.02.011.

References

[1] M.M. Abu-Khader, Prog. Nucl. Energy 51 (2009) 225–235.
[2] X. Sun, H. Luo, S. Dai, Chem. Rev. 112 (2012) 2100–2128.
[3] C.L. Xiao, C.Z. Wang, L.Y. Yuan, et al., Inorg. Chem. 53 (2014) 1712–1720.
[4] R.A. Peterson, E.C. Buck, J. Chun, et al., Environ. Sci. Technol. 52 (2018) 381–396.
[5] B.J. Mincher, The nuclear renaissance: producing environmentally sustainable nuclear power, in: C.M. Wai, B.J. Mincher (Eds.), Nuclear Energy and the Environment, Washington, DC, 2010, pp. 3-10.
[6] C. Xiao, Z. Hassanzadeh Fard, D. Sarma, et al., J. Am. Chem. Soc. 139 (2017) 16494–16497.
[7] S.A. Ansari, P. Pathak, P.K. Mohapatra, V.K. Manchanda, Sep. Purif. Rev. 40 (2011) 43–76.
[8] W. Jianchen, S. Chongli, Solvent Extr. Ion Exch. 19 (2001) 231–242.
[9] C. Madic, B. Boullis, P. Baron, et al., J. Alloys Compd. 444-445 (2007) 23–27.
[10] J. Veliscek-Carolan, J. Hazard. Mater. 318 (2016) 266–281.
[11] N.M. Edelstein, J. Fuger, J.J. Katz, L.R. Morss, Summary and comparison of properties of the actinide and transactinide elements, in: L.R. Morss, N.M. Edelstein, J. Fuger (Eds.), The Chemistry of the Actinide and Transactinide Elements, Springer Netherlands, Dordrecht, 2011, pp. 1753–1835.
[12] M.J. Hudson, L.M. Harwood, D.M. Laventine, F.W. Lewis, Inorg. Chem. 52 (2013) 3414–3428.
[13] P.R. Zalupski, D.D. Ensor, C.L. Riddle, D.R. Peterman, Solvent Extr. Ion Exch. 31 (2013) 430–441.
[14] M. Weigl, A. Geist, U. Müllich, K. Gompper, Solvent Extr. Ion Exch. 24 (2006) 845–860.
[15] B.B. Beele, U. Müllich, F. Schwörer, A. Geist, P.J. Panak, Procedia Chem. 7 (2012) 146–151.
[16] D. Magnusson, B. Christiansen, R. Malmbeck, J.P. Glatz, Radiochim. Acta 97 (2009) 497–502.
[17] D. Magnusson, B. Christiansen, M.R.S. Foreman, et al., Solvent Extr. Ion Exch. 27 (2009) 97–106.
[18] S.Y. Ning, X.P. Wang, Q. Zou, et al., Sci. Rep. 7 (2017) 14679.
[19] Y. Li, X. Dong, J. Yuan, et al., Inorg. Chem. 59 (2020) 3905–3911.
[20] Y. Li, X. Yang, P. Ren, et al., Inorg. Chem. 60 (2021) 5131–5139.
[21] A. Khayambashi, Q. Shu, Y. Wei, F. Tang, L. He, J. Radioanal. Nucl. Chem. 316 (2018) 221–231.
[22] Q. Shu, A. Khayambashi, Q. Zou, et al., J. Radioanal. Nucl. Chem. 313 (2017) 29–37.
[23] J.S. Fritz, J. Am. Chem. Soc. 122 (2000) 12411–12412.
[24] F. Zha, X. Wang, X. Wang, et al., J. Radioanal. Nucl. Chem. 311 (2017) 1793–1802.
[25] S. Usuda, Y. Wei, Y. Xu, et al., J. Nucl. Sci. Technol. 49 (2012) 334–342.
[26] S. Ning, Q. Zou, X. Wang, R. Liu, Y Wei, Sci. China Chem. 59 (2016) 862–868.
[27] Y. Wei, M. Kumagai, Y. Takashima, G. Modolo, R. Odoj, Nucl. Technol. 132 (2000) 413–423.
[28] S. Ning, Q. Zou, X. Wang, R. Liu, Y. Wei, J. Nucl. Sci. Technol. 53 (2016) 1417–1425.
[29] S. Ning, X. Wang, R. Liu, et al., J. Radioanal. Nucl. Chem. 303 (2015) 2011–2017.
[30] S. Demir, N.K. Brune, J.F. Van Humbeck, et al., ACS Cent. Sci. 2 (2016) 253–265.
[31] J.A. Shusterman, H.E. Mason, J. Bowers, et al., ACS Appl. Mater. Interfaces 7 (2015) 20591–20599.
[32] W. Zhang, X. He, G. Ye, R. Yi, J. Chen, Environ. Sci. Technol. 48 (2014) 6874–6881.
[33] M.A. Higginson, O.J. Marsden, P. Thompson, F.R. Livens, S.L. Heath, React. Funct. Polym. 91-92 (2015) 93–99.
[34] S. Das, P. Heasman, T. Ben, S. Qiu, Chem. Rev. 117 (2017) 1515–1563.
[35] K. Geng, T. He, R. Liu, et al., Chem. Rev. 120 (2020) 8814–8933.
[36] Y. Tian, G. Zhu, Chem. Rev. 120 (2020) 8934–8986.
[37] T. Zhang, G. Xing, W. Chen, L. Chen, Mater. Chem. Front. 4 (2020) 332–353.
[38] P. Wu, H. Liu, M. Sun, et al., J. Mater. Chem. A 9 (2021) 27320–27331.
[39] J.K. Sun, Q. Xu, Energy Environ. Sci. 7 (2014) 2071–2100.
[40] X. Zou, H. Ren, G. Zhu, Chem. Commun. 49 (2013) 3925–3936.
[41] U. Díaz, A. Corma, Coord. Chem. Rev. 311 (2016) 85–124.
[42] F.W. Lewis, L.M. Harwood, M.J. Hudson, et al., Inorg. Chem. 52 (2013) 4993–5005.
[43] M.A. Higginson, N.D. Kyle, O.J. Marsden, et al., Dalton Trans. 44 (2015) 16547–16552.
[44] F.W. Lewis, L.M. Harwood, M.J. Hudson, et al., J. Am. Chem. Soc. 133 (2011) 13093–13102.
[45] Y. Jin, Y. Zhu, W. Zhang, CrystEngComm 15 (2013) 1484–1499.
[46] X. Sun, N. Wang, Y. Xie, et al., Talanta 225 (2021) 122072.
[47] H.L. Nguyen, C. Gropp, Y. Ma, C. Zhu, O.M. Yaghi, J. Am. Chem. Soc. 142 (2020) 20335–20339.
[48] M. Zhang, H. Liu, T. Ma, Z. Song, S. Shao, Chem. Eng. J. 403 (2021) 126379.
[49] L. He, S. Liu, L. Chen, et al., Chem. Sci. 10 (2019) 4293–4305.
[50] R. Khatoon, Y. Guo, S. Attique, et al., J. Alloys Compd. 837 (2020) 155294.
[51] Y. Liu, X. Yang, S. Ding, et al., Inorg. Chem. 57 (2018) 5782–5790.
[52] S. Trumm, A. Geist, P.J. Panak, T. Fanghänel, Solvent Extr. Ion Exch. 29 (2011) 213–229.
[53] in F. Deng, X.B. Luo, L. Ding, S.L. Luo, Application of nanomaterials and nanotechnology in the reutilization of metal ion from wastewater, in: X. Luo, F. Deng (Eds.), Nanomaterials for the Removal of Pollutants and Resource Reutilization Elsevier, Amsterdam, 2019, pp. 149–178.
[54] S. Ploychompoo, Q. Liang, X. Zhou, C. Wei, H. Luo, Phys. E 125 (2021) 114377.
[55] Y. Karslyan, F.V. Sloop, L.H. Delmau, et al., RSC Adv. 9 (2019) 26537–26541.
[56] C. Adam, P. Kaden, B.B. Beele, et al., Dalton Trans. 42 (2013) 14068–14074.
[57] A.L. Goodman, E.T. Bernard, V.H. Grassian, J. Phys. Chem. A 105 (2001) 6443–6457.